Journal of the European Ceramic Society 42 (2022) 4006–4015

Contents lists available at ScienceDirect

Journal of the European Ceramic Society

journal homepage: www.elsevier.com/locate/jeurceramsoc

Manganese crystalline phases developed in high lead glazes during firing

J. Molera [a,*], M. Colomer [b], O. Vallcorba [c], T. Pradell [d]

[a] MECAMAT, Facultat de Ciències i Enginyeries. Universitat de Vic – Universitat Central de Catalunya, C. de la Laura, 13, 08500 Vic, Spain
[b] Universitat de Barcelona, Dept. Educació Lingüística i Literària, i Didàctica de les Ciències Experimentals i de la Matemàtica Campus Mundet, Passeig de la Vall d'Hebron, 171, 08035 Barcelona, Spain
[c] ALBA Synchrotron Light Source, Carrer de la Llum 2-26, 08290 Cerdanyola del Vallès, Barcelona, Spain
[d] Universitat Politècnica de Catalunya BarcelonaTech, Departament de Física, BRCMSE, Campus Diagonal-Besòs, Av. Eduard Maristany 10-14, 08019 Barcelona, Spain

ARTICLE INFO

Keywords:
High temperature synchrotron powder X-ray diffraction
High lead glaze
$PbO-SiO_2-MnO-Al_2O_3-MgO-CaO$
Barysilite
Kentrolite
Braunite
Ganomalite
Margarosanite

ABSTRACT

A High Temperature Synchrotron Radiation X-Ray Powder Diffraction experiment was performed to determine the manganese compounds formed during the heating and cooling of 70 wt% PbO – 30 wt% SiO2 mixture or the equivalent glass plus 10 wt% of MnO. The effect of adding calcite, dolomite and kaolinite were also studied. All mixtures were fired between 690 °C and 1020 °C in oxidizing conditions and analysed by Scanning Electron Microscopy.

A sequence of manganese phases are formed during firing: bixbyite (Mn_2O_3), barysilite ($(Pb,Mn)Si_2O_7$), kentrolite ($Pb_2Mn_2Si_2O_9$) and braunite (Mn_7SiO_{12}). Kentrolite and braunite crystallise with different crystal habits during the heating and the cooling. If dolomite is present diopside ($(Ca,Mg,Mn)_2Si_2O_6$) is formed. If calcite is present, ganomalite ($Pb_3(CaMn)_2Si_3O_{11}$), margarosanite ($Pb(Ca,Mn)_2Si_3O_9$) and wollastonite ($(Ca,Mn)SiO_3$) are also formed. Wollastonite can incorporate enough manganese to transform into bustamite ($(Mn,Ca)_3Si_3O_9$) at high temperatures. This leaves less manganese available for the crystallisation of kentrolite and braunite.

1. Introduction

Manganese oxides were used since antiquity as glaze ceramic brown/black pigments. In most of the cases, manganese oxide dissolves into the glaze but it is not uncommon to found manganese crystalline compounds associated to the dark decorations in historical ceramics. Kentrolite ($Pb_2Mn_2Si_2O_9$), hausmannite (Mn_3O_4) and braunite (Mn_7SiO_{12}) crystals are found in Islamic tin-lead-glazed pottery [1,2]. Kentrolite and hausmannite are found in Hispano moresque pottery [3], in the oldest Swiss tin-opacified stove tiles [4] and in 16th century Portuguese productions [5]. Bustamite ($(Mn,Ca)_3Si_3O_9$) is found in medieval 10th century production in la Vega de Granada [6], 14–15th century Portugal [7] and 13–14th century Barcelona productions [1,2]. Braunite only is found in 17th century tin-lead glazes from Portugal, Barcelona and Hungary [1,3,8,9] among others.

The nature, size and distribution of the manganese crystals depends on the composition of the pigment, glaze and ceramic substrate and firing protocol. MnO reacts with PbO and SiO_2 and may produce manganese oxides (bixbyite, haussmanite), silicates (braunite) and lead silicates (kentrolite). However, CaO, MgO and Al_2O_3 are also commonly present in the high-lead glazes, either in the glass initial components or due to the reaction of the melt with the ceramic. They are commonly present as calcite, dolomite and clay or feldspar among others. Their incorporation increases the stability of the glaze but, it also gives rise to the precipitation of crystalline phases such as calcium and magnesium silicates and aluminosilicates (wollastonite, $CaSiO_3$, diopside, $CaMgSi_2O6$ and lead feldspar, $PbAl_2Si_2O_8$), some of which are known to incorporate manganese in the structure (wollastonite, bustamite, diopside).

As kentrolite tend to dissolve at ~950 °C [10] some attempts have been made based on the equilibrium phase diagrams available to correlate their presence with the firing temperature followed in historical glazed wares [1,8,11]. Even though the $PbO-SiO_2-MnO$ phase diagram does not exist, some other phase diagrams, such as $PbO-SiO_2$ [12–15], $PbO-SiO_2-CaO$ [16–18], $PbO-SiO_2-Al_2O_3$ [19], SiO_2-MnO [20,21] and $CaO-MnO-SiO_2$ [21,22] do and can give only partial information about the compounds that may form.

Furthermore, high lead glazes were obtained either using lead compounds and quartz or a lead-glass. In the former case, many phases are produced during the heating, before the glaze melt and, in both cases, some phases may also be obtained during the cooling. Which manganese compounds are formed in each case and, whether they are

* Corresponding author.
E-mail address: judit.molera@uvic.cat (J. Molera).

https://doi.org/10.1016/j.jeurceramsoc.2022.03.028
Received 14 December 2021; Received in revised form 5 March 2022; Accepted 15 March 2022
Available online 17 March 2022

Table 1
Calculated chemical composition of the mixtures (wt%). SiO_2 is added as quartz, PbO as minium or massicot/litharge, MnO as manganosite, CaO as calcite, MgO as dolomite and Al_2O_3 as kaolinite. *Glass(70%PbO+30%SiO_2) + MnO.

REF.	PbO	SiO_2	Al_2O_3	CaO	MgO	MnO
R7	63.1	27.7				9.2
R7-C	60.0	26.3		4.9		8.8
R7-D	60.2	26.4		2.7	1.9	8.8
G7 *	63.1	27.7				9.2
KR7	58.1	28.2	4.3			9.4
KR7-C	55.2	26.8	4.1	5.0		8.9
KR7-D	55.4	26.9	4.1	2.7	2.0	8.9
R8	72.7	18.2				9.1

produced during the heating or during the cooling is not known. In fact, kentrolite crystallites with different shapes have been found in some historical glazes. Some, growing around the manganese oxide particles with prismatic shape and some with a needle like shape [4,8]. The later have been related to a possible fast-cooling process. Braunite crystallites also show two different morphologies in 17th century Catalan brown decorated ware: dark brown bipyramidal crystallites and brown thin lath-like crystallites [8].

The object of this study is to investigate the manganese compounds formed during the firing of a high-lead glaze and their possible role as a fingerprint of the materials and firing conditions used in the production of manganese decorated lead glazes. For this, a High Temperature Powder X-Ray Diffraction (HT-PXRD) experiment with Synchrotron Radiation has been designed to determine the phases formed and their stability range during the heating and cooling. Several mixtures of manganese oxide with lead oxide and quartz with a near eutectic high-lead glass composition to which calcite, dolomite and kaolinite were added, are studied. A mixture of manganese oxide with a 70PbO:30SiO_2 glass is also studied.

The same mixtures were fired between 690 °C and 1020 °C following the same thermal path in a kiln at the laboratory. The resulting glazes were analysed by Scanning Electron Microscopy (SEM).

2. Experimental methodology

A basic mixture of near eutectic composition high-lead glass, 70 wt% PbO:30 wt% SiO_2, with addition of 10 wt% MnO, labelled **R7**, was prepared using minium (Pb_3O_4, Panreac 121476.1211), quartz (SiO_2, Sigma 101194530) and manganosite (MnO, Panreac 211408.1210), see Table 1 for exact composition in oxides compounds.

To study the effect of CaO, MgO and Al_2O_3 in the manganese phases developed we added calcite, dolomite and kaolinite to the R7 mixture. A mixture of R7 with 10 wt% calcite ($CaCO_3$, Panreac 121212.1210) labelled **R7-C** and a mixture of R7 with 10 wt% dolomite ($CaMg(CO_3)_2$, FAST ANCIL) labelled **R7-D** have been obtained. Furthermore, 10% of kaolinite ($Al_2Si_2O_5(OH)_4$, FAST ANCIL), has also been added to the R7 mixture and labelled **KR7**. Calcite and dolomite have also been added to the KR7 mixture and the corresponding mixtures labelled **KR7-C** and **KR7-D** respectively.

To solve the question regarding what happens when a lead glass is used instead of a mixture of quartz and lead compounds, a 70 wt% PbO:30 wt% SiO_2 glass was molten in an alumina crucible at 980 °C for 1 h. Only the central part of the glass was used to avoid, as far as possible, the reaction with the crucible walls. A mixture of the ground glass with 10 wt% of MnO (MnO, Panreac 211408.1210) was also prepared (labelled **G7**).

Finally, a lead richer mixture of composition 80 wt% PbO:20 wt% SiO_2 with 10 wt% of MnO, labelled **R8**, was also prepared using (PbO, 203610 Sigma-Aldrich) quartz and 10% g of manganosite. This mixture was prepared to study what happens in lead richer glazes.

The mixtures were ground in an agate mortar down to a final granulometry below 80 μm before inserting them into a 500 μm diameter quartz capillary for the high-temperature synchrotron powder X-ray diffraction experiment (HT-XRPD). The use of coarser ground materials will only slow down the decomposition and will shift up the transformation temperatures. We are interested in determining the sequence of phases formed in conditions which are not limited by the kinetics of the transformation. For this reason, we should use a finely ground material.

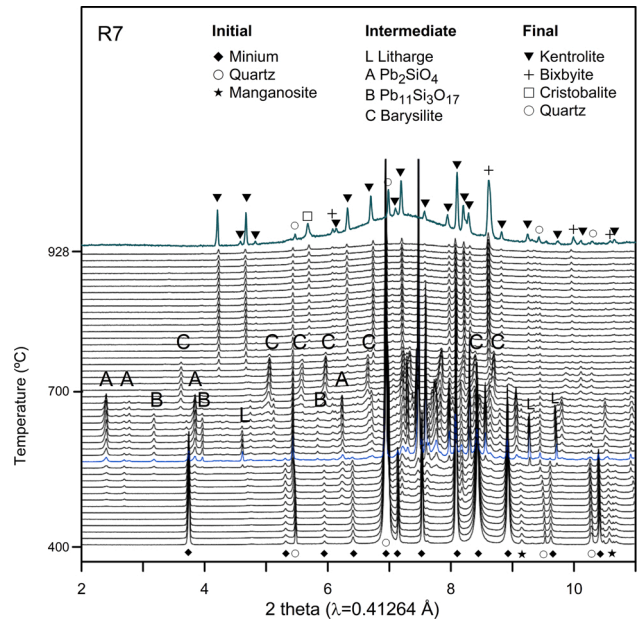

Fig. 1. PXRD sequence corresponding to the R7 mixture showing the evolution of the phases during the heating. The blue XRD pattern corresponds to the α to β quartz transition (573 °C). The last pattern on top was taken after cooling.

measurements were performed in transmission mode while rotating the capillary to improve particle statistics at an energy of 30 keV (wavelength λ = 0.41264 Å determined from a Si640d NIST standard), to minimize the strong absorption of lead containing mixtures. Diffraction data were collected by a 6-module Mythen detector covering an angular range of 40° (2θ) with a stepsize of 0.006°. A FMB Oxford hot air blower was used to heat from room temperature (RT) to 400 °C at 20 °C/min, from 400 °C to 928 °C at 10 °C/min and cool down from 928 to RT at 25 °C/min. The blower temperature was calibrated from the Si640d NIST cell parameter refined from diffraction data collected at the same conditions as the samples. The maximum temperature that could be reached was 928 °C. During the heating and cooling stages data collection was performed sequentially with an acquisition time of 10 s. The final temperatures (928 °C and RT) were maintained for 5 min.

To study the microstructure developed during firing at different firing temperatures and also at a higher temperature than the 928 °C reached in the HT-PXRD experiment, the mixtures were applied over an already fired tile ceramic support and fired at 690 °C, 740 °C, 800 °C, 850 °C, 928 °C, 950 °C, 980 °C and 1020 °C. The firing was performed using the same heating ramp of 10 °C/min keeping the maximum temperature for 10 min. The surface was studied by scanning electron microscopy (SEM). A crossbeam workstation (Zeiss Neon 40; Carl Zeiss AG, Oberkochen, Germany) equipped with a Schottky field emitter column with an Energy Dispersive Spectroscopy (EDS) detector (INCAPentaFETx3 detector, 30 mm^2, ATW2 window, Oxford Instruments, Abingdon, UK) attached was employed for the SEM investigation. Backscattered electron (BSE) images were obtained and the crystallites formed were analysed to determine their composition at 20 kV acceleration voltage with 20 nA current, 7 mm working distance and 120 s measuring time. The EDS is calibrated using oxides and mineral standards and a high lead glass (K229, Geller Microanalytical Laboratory, MA, USA).

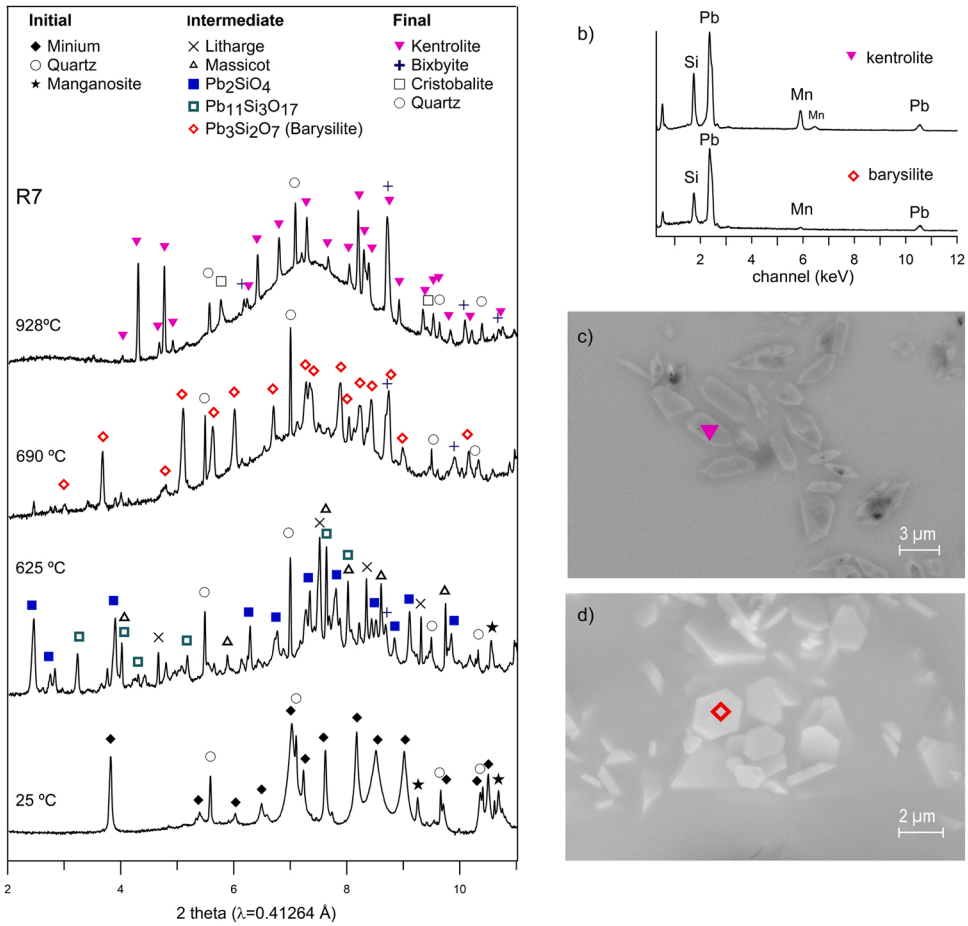

Fig. 2. (a) Selection of PXRD patterns taken at different temperatures showing the main phases formed in the R7 mixture. (b) EDS spectra and BSE images from (c) kentrolite and (d) barysilite crystals formed firing at 850 °C and 740 °C respectively.

The glazes surface was also analysed by conventional XRD, a Bruker D8 Advance Bragg-Brentano with a PSD Lynx-Eye detector with monochromator, using Cu Kα radiation (wavelength $\lambda = 1.5418$ Å).

XRD Phase identification was performed using the International Centre for Diffraction Data (ICDD) PDF-4 Database. A list of the compounds identified and the corresponding files are given in the supplementary materials (Table S1).

3. Results

3.1. R7, R8 and G7 mixtures

The transformations happening in the PbO-SiO_2-MnO mixtures, **R7** and **R8**, during the HT-PXRD experiment are shown in Fig. 1 and Fig. S1. In both mixtures, manganosite (MnO) transforms to bixbyite (Mn_2O_3) at 520 °C and 580 °C for **R7** and **R8** respectively. Minium (Pb_3O_4) transforms to litharge/massicot (PbO) between 560 and 590 °C which disappears at ≈ 650 °C for **R7** and 670 °C for **R8**. In parallel, lead oxide reacts with quartz producing first lead rich silicates, hexagonal Pb_2SiO_4 at ≈ 500 °C and then, monoclinic Pb_2SiO_4 and $Pb_{11}Si_3O_{17}$ at ≈ 510 °C which melt below 700 °C. A silica richer lead silicate, barysilite ($Pb_{2.8}Mn_{0.2}Si_2O_7$), forms at ≈ 650 °C and melts at ≈ 750 °C. Bixbyite reacts with the melt formed and kentrolite ($Pb_2Mn_2Si_2O_9$) crystallises around the manganese oxide particles at above 700 °C. Quartz does not react completely and, a small part of it transforms into cristobalite at about 760–800 °C. The crystallisation of cristobalite at such low temperatures and as soon as a silicate liquid is formed has already been observed and its metastability associated to the presence of other elements than silica in the melt, such as, sodium, lead [23,24] or iron [25].

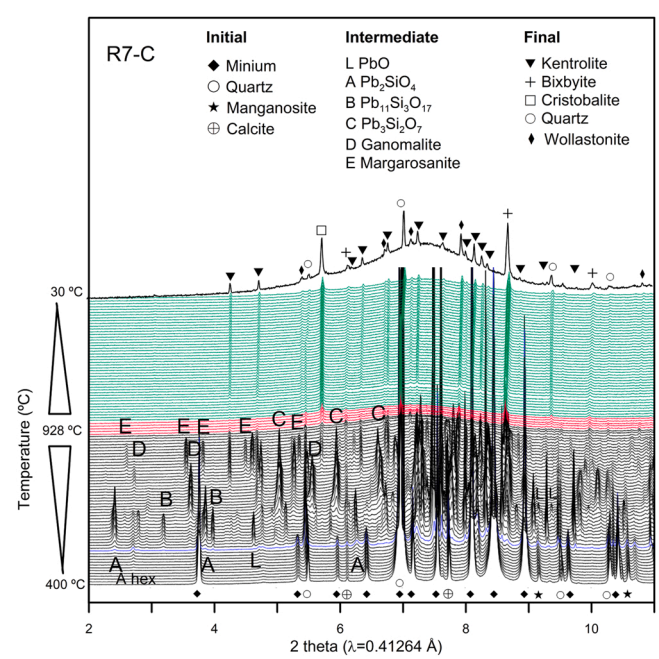

Fig. 3. Heating (black) and cooling (green) PXRD sequence corresponding to the R7-C mixture showing the evolution of the phases during the thermal cycle. In red the XRD patterns taken during the maximum temperature (928 °C) stage.

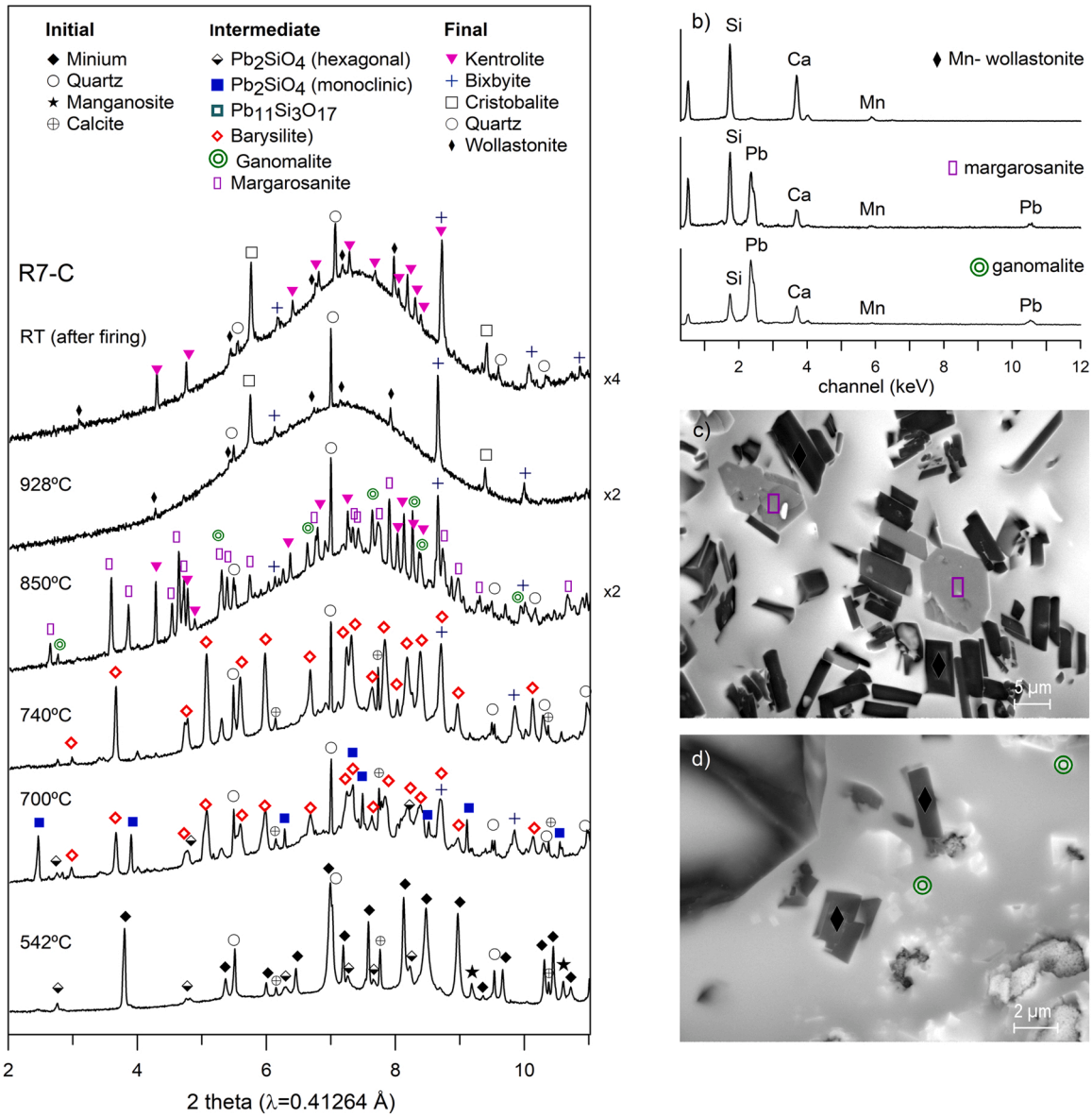

Fig. 4. (a) Selection of PXRD patterns taken at different temperatures showing the main phases formed in the R7-C mixture. (b) EDS spectra and BSD images from (c) Mn-wollastonite and margarosanite formed firing at 850ºC and (d) and ganomalite crystals formed firing at 800 °C.

A selection of HT-PXRD patterns taken at different temperatures and SEM-BSE images of the hexagonal crystals of barysilite and prismatic crystals of kentrolite are shown in Fig. 2.

When the glass, **G7**, is fired, manganosite is also partially transformed into bixbyite but at a higher temperature ≈ 630 °C and then into kentrolite at ≈ 670 °C. At this temperature the glass is already behaving as a liquid, and therefore, kentrolite is also obtained from the reaction of the manganese oxide with the silicate melt. Cristobalite is also formed at ≈ 700 °C from some unreacted quartz present in the glass.

3.2. R7-C and R7-D Mixtures

The addition of calcite or dolomite to the raw mixture does neither change the lead silicates and manganese oxides phases formed nor the temperature range of the transformations.

Nevertheless, new phases appear following the decomposition of calcite and dolomite at ≈ 830 °C and ≈ 790 °C respectively. Fig. 3 shows the phases formed in the **R7-C** mixture. Lead and calcium silicates are formed. Calcium barysilite ($Pb_{2.4}Ca_{0.5}Mn_{0.1}Si_2O_7$) is found between ≈ 675 °C and ≈ 830 °C, ganomalite ($Pb_3Ca_{1.9}Mn_{0.1}Si_3O_{11}$) between≈ 720 °C and ≈ 860 °C, kentrolite between ≈ 760 °C and ≈ 928 °C, margarosanite ($PbCa_{1.9}Mn_{0.1}Si_3O_9$) between ≈ 790 °C and ≈ 915 °C and Mn-wollastonite ($Ca_{2.8}Mn_{0.2}Si_3O_9$) between ≈ 900 °C and ≈ 928 °C. A selection of HT-PXRD patterns taken at different temperatures and SEM-BSE images of crystals of margarosanite, ganomalite and Mn-wollastonite are shown in Fig. 4.

As soon as dolomite decomposes in the **R7-D** mixture, ≈ 800 °C, Mn-diopside ($Ca_{0.9}Mg_{0.9}Mn_{0.2}Si_2O_6$) is formed instead of wollastonite, Fig. S1. This is in agreement with Fröberg et al. works [26] that showed the influence of CaO content in CaO-MgO-Al_2O_3-SiO_2 system and pointed out that when MgO:CaO > 0.2 the glaze was composed of diopside crystals, MgO:CaO ≈ 0.2 resulted in the combined crystallisation of diopside and wollastonite ($CaSiO_3$) and when MgO:CaO < 0.2 gave only wollastonite. The amount of quartz also seemed to influence the precipitation of wollastonite and diopside. If the quartz content was low, only diopside was observed, thus suggesting that all the quartz available is consumed in diopside formation [27].

Finally, cristobalite is also formed at ≈ 800 °C in both mixtures. One

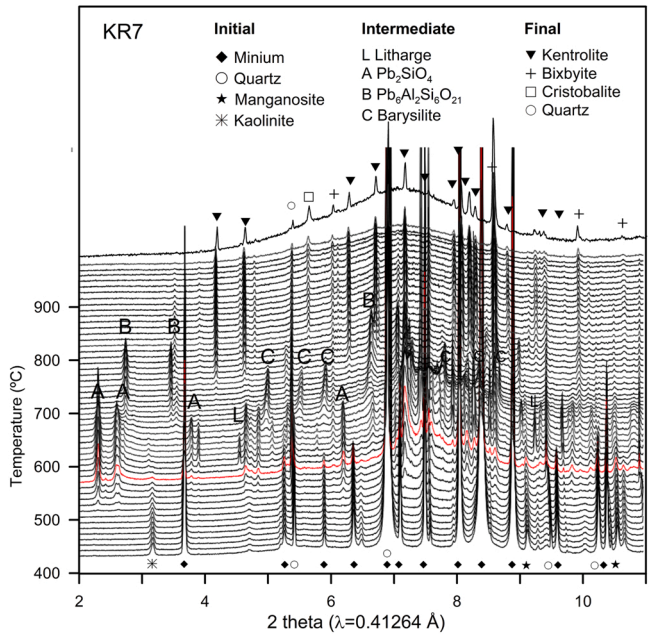

Fig. 5. PXRD sequence corresponding to the KR7 mixture showing the evolution of the phases during the heating. The red XRD pattern corresponds to the α to β quartz transition (573 °C). The last pattern on top was taken after cooling.

interesting difference with respect to the calcite and dolomite free mixture **R7** is that the kentrolite XRD-peaks disappear at the maximum temperature reappearing during the cooling, at 780 °C and 870 °C for **R7-C** and **R7-D** respectively.

3.3. KR7, KR7-C, KR7-D mixtures

When kaolinite is added to the **R7** mixture (**KR7**), lead aluminosilicates are formed in addition to the lead silicates previously found, Pb_2SiO_4, $Pb_{11}Si_3O_{17}$ and barysilite ($Pb_8Mn(Si_2O_7)_3$), Fig. 5. A lead rich lead aluminosilicate, $Pb_8Al_2Si_4O_{19}$ is found between ≈ 500 °C and ≈ 720 °C, followed by lead poorer lead aluminosilicates, $Pb_6Al_2Si_6O_{21}$, between ≈ 670 °C and ≈ 820 °C and lead feldspar ($PbAl_2Si_2O_8$) between ≈ 760 °C and ≈ 928 °C. During the high temperature stage (928 °C) the lead feldspars melt. Kentrolite forms at 730 °C and is kept during the cooling.

In the mixtures containing also calcite (**KR7-C**) or dolomite (**KR7-D**) only the lead richer lead aluminosilicate ($Pb_8Al_2Si_4O_{19}$) is found between ≈ 520 °C and ≈ 730 °C (Fig. S1). Calcium barysilite ($Pb_{2.5}Ca_{0.4}Mn_{0.1}Si_2O_7$) is found between ≈ 600 °C and ≈ 825 °C in **KR7-C** and between ≈ 625 °C and ≈ 800 °C in **KR7-D**. Manganoan wollastonite ($Ca_{2.8}Mn_{0.2}Si_3O_9$) is formed at 850 °C in **KR7-C** and Mn-diopside ($Ca_{0.9}Mg_{0.9}Mn_{0.2}Si_2O_6$) at ≈ 800 °C in **KR7-D.** Curiously, when calcite or dolomite are added, only the lead richest aluminosilicate is obtained, and, lead feldspar is not found.

A selection of HT-PXRD patterns from **KR7-D** taken at different temperatures and SEM-BSE images of Mn-diopside, barysilite and kentrolite crystals are shown in Fig. 6.

3.4. Transformations above 928 °C

The evolution of the phases formed during heating and cooling in the HT-PXRD experiments are shown in Fig. 7. We can see that, during the heating and approaching 900 °C, kentrolite decreases in **R7**, **R8**, **G7, KR7, R7-C** and **R7-D** and disappears during the maximum temperature stage at 928 °C in **R7-C** and **R7-D**. Subsequently, during the cooling, kentrolite recrystallises (Fig. 7). In contrast, kentrolite melts at 920 °C but does not recrystallise during the cooling in **KR7-C** and **KR7-D**.

Although in the HT-PXRD experiment a temperature higher than 928 °C could not reached, the same mixtures were also fired in the laboratory at 928 °C, 950 °C, 980 °C and 1020 °C and studied by OM and SEM-EDS and conventional XRD. SEM-BSD and/or Optical images were obtained, and the crystallites analysed, Fig. 8.

In all the mixtures, kentrolite recrystallises during the cooling with a very characteristic feather like crystal habit in all the mixtures. We can see that kentrolite is abundant at 928 °C and 950 °C in **R7** and **KR7** while is scarce in the other. A few crystals are still found at 980 °C in **R7-C**. Few tiny square crystals of braunite (Mn_7SiO_{12}) are observed already at 928 °C, growing and developing tails at the vertices at higher temperatures. The shape, size and extension of braunite is remarkable in **R7** and **KR7** above 980 °C where large dendritic crystals or clusters of smaller crystals occupy large areas of the glazes.

The Mn-wollastonite formed in the calcitic mixtures (**R7-C** and **KR7-C**) becomes Mn richer at higher temperatures, $Ca_{2.7}Mn_{0.3}Si_3O_9$ at 980 °C and $Ca_{1.8}Mn_{1.2}Si_3O_9$ at 1020 °C. Wollastonite and bustamite ($Mn_xCa_{2.4-x}Si_3O_9$) are pyroxenoids with structures derived from variations in the stacking sequence of a single type of structural unit [28], with similar XRD patterns. The composition of the crystallites obtained after firing at 1020 °C agrees with bustamite [29] (Fig. S2). In the dolomitic mixtures (**R7-D** and **KR7-D**), Mn-diopside crystallites formed becoming also manganese richer at 1020 °C ($Ca_{0.7}Mg_{0.8}Mn_{0.5}Si_2O_6$).

Moreover, in the calcitic and dolomitic mixtures (**R7-C**, **KR7-C**, **R7-D** and **KR7-D**), small crystallites of braunite are formed, some at the surface of bustamite at 1020 °C and of Mn-diopside at 980 °C. The small size can be related to the diminished amount of manganese in the glass/melt available due to the incorporation of manganese in the wollastonite/bustamite/diopside.

4. Discussion

The data obtained has shown that the manganese oxide phase determined at a temperature ≈ 550 °C in all the cases is bixbyite (Mn_2O_3). From the reaction of lead oxide and quartz, a sequence of lead rich silicates is formed ending in barysilite ($(Pb,Mn)Si_2O_7$) which incorporates some manganese (> 625 °C) and disappearing completely at 830 °C. In the mixtures with calcite or dolomite, barysilite incorporates also calcium in the structure. In the mixtures with kaolinite, lead alumino-silicates are also formed.

Kentrolite ($Pb_2Mn_2Si_2O_9$) is formed above 700 °C from the reaction of bixbyite (Mn_2O_3) with the lead-silicate melt. The lead-silicate melt forms from the raw compounds (lead oxide plus quartz, R7) at about 700 °C and the lead-silicate glass (G7) behaves like a high viscous liquid already at the glass transition temperature (≈500 °C). Consequently, kentrolite forms at a slightly higher temperature in the former (>700 °C) than in the latter (≈670 °C). In the calcitic and dolomitic mixtures, kentrolite is formed at higher temperatures, > 750 °C.

Although kentrolite melts at a temperature close to the maximum temperature reached in the HT-PXRD experiments, 928 °C, it recrystallises during the cooling. The shape and size of the kentrolite crystallites formed in the heating is different than those formed in the cooling. During the heating, small bipyramidal crystallites grow around the manganese oxide grains. During the cooling, large feather-like crystallites are formed (Fig. 8). Feather-like crystallites of kentrolite are found in the mixtures fired at 928 °C and 950 °C and, also for the calcitic lead-silica mixture (**R7-C**) at 980 °C. At 1020 °C kentrolite is not able to form again during the cooling in any mixture.

At 928 °C kentrolite ($Pb_2Mn_2Si_2O_9$) and bixbyite (Mn_2O_3) melt and a manganese-rich-liquid is formed, in this liquid, braunite (Mn_7SiO_{12}) crystallises (Fig. 8). Few small crystals of braunite could be seen by OM and SEM-EDS in samples fired at 928 °C in the laboratory even though they were no detected by XRD. In the calcium and magnesium free mixtures (**R7** and **KR7**), braunite crystallises first as individual small squares with long tails, then, at a higher temperature, also as dendritic growths forming Christmas trees.

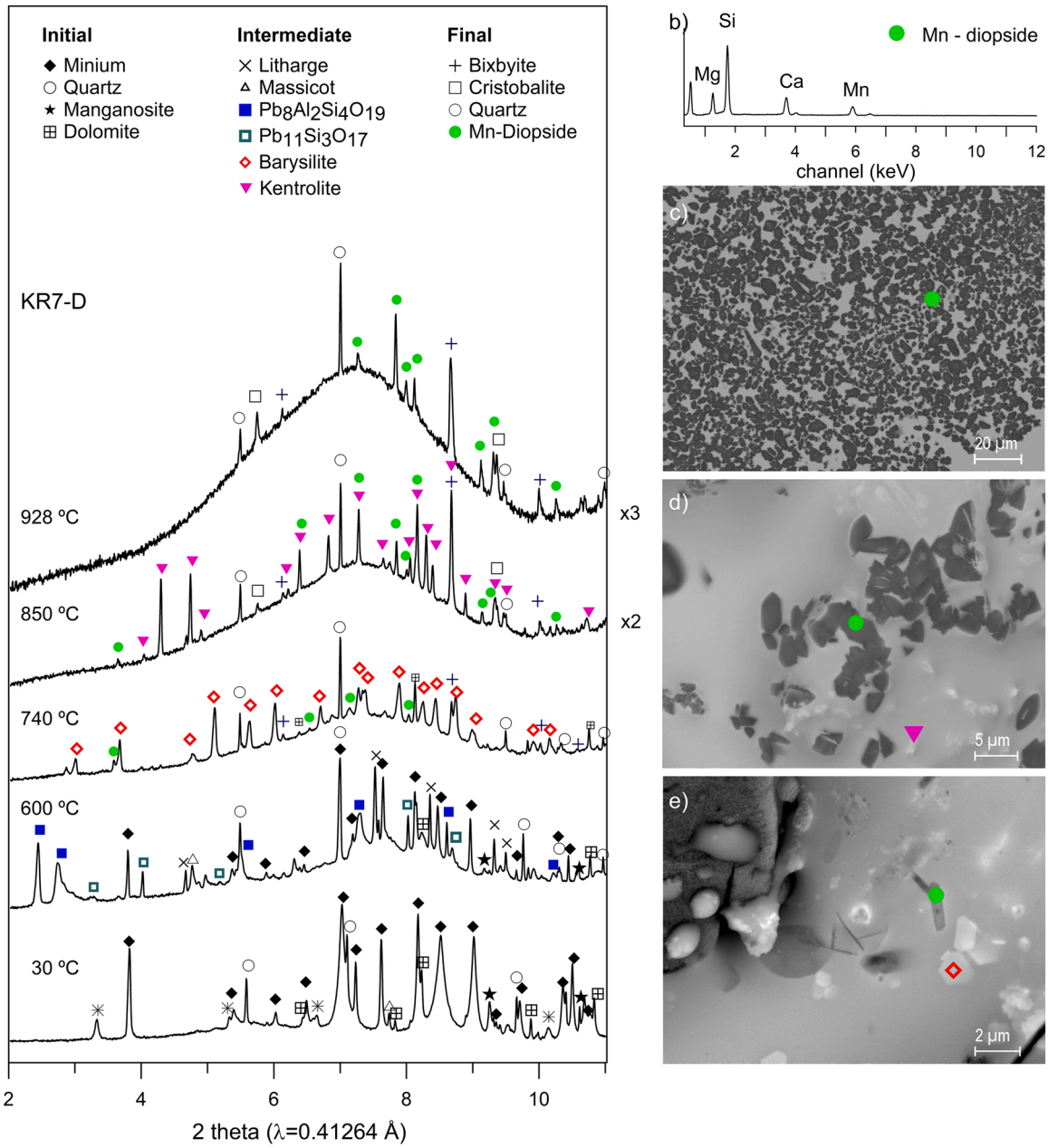

Fig. 6. (a) Selection of PXRD patterns taken at different temperatures showing the main phases formed in the KR7-D mixture. (b) EDS spectrum of Mn-diopside and BSE images from the phases formed at (c) 928 °C (d) 850 °C and (e) 740 °C.

Bixbyite (Mn_2O_3), braunite (Mn_7SiO_{12}) and neltnerite ($CaSiMn_6O_{12}$) are members of a polysomatic series with general formula $(Mn,X)_8O_{12}$ with X = Si or Ca [11,30]. Bixbyite and braunite have very similar XRD patterns but can be identified by SEM-EDS. We have not found neltnerite in the calcitic mixtures.

In the calcitic mixture **R7-C**, calcium lead silicates are formed, ganomalite ($Pb_3(CaMn)_2Si_3O_{11}$) between ≈ 720 °C and ≈ 860 °C and margarosanite ($Pb(Ca,Mn)_2Si_3O_9$) between ≈ 790 °C and ≈ 915°C while margarosanite is not formed in **KR7-C**, both phases incorporate manganese. At higher temperature Mn-wollastonite predominates. In the dolomitic mixtures, (**R7-D**, **KR7-D**) only Mn-diopsides are formed.

In the calcitic and dolomitic mixtures (**R7-C**, **R7-D**, **KR7-C**, **KR7-D**), the formation of Mn-wollastonite or Mn-diopside leaves less manganese available in the melt and, consequently, only tiny crystallites of braunite are formed growing also around the Mn-wollastonite and Mn-diopside crystallites (Fig. 8). The braunite crystallites are small but, at high temperature, 1020 °C, may show also dendritic growths. SEM images show that braunite crystals form clusters with larger crystals at the periphery and small crystals at the centre. This clusters are related to the immiscibility between the manganese rich and manganese poor liquids resulting from the melting of kentrolite ($Pb_2Mn_2Si_2O_9$) and bixbyite (Mn_2O_3). Braunite (Mn_7SiO_{12}) crystals show also very different shapes, tiny square crystals are most probably formed during the heating while the tails and dendritic growths during the cooling.

5. Conclusions

Manganese oxide is a common compound used to colour and decorate historical glazed wares. Many different manganese phases have been identified in traditional high-lead glazes and their presence must be related to the materials used and firing protocol. The object of the study was to investigate their possible role as a fingerprint of the

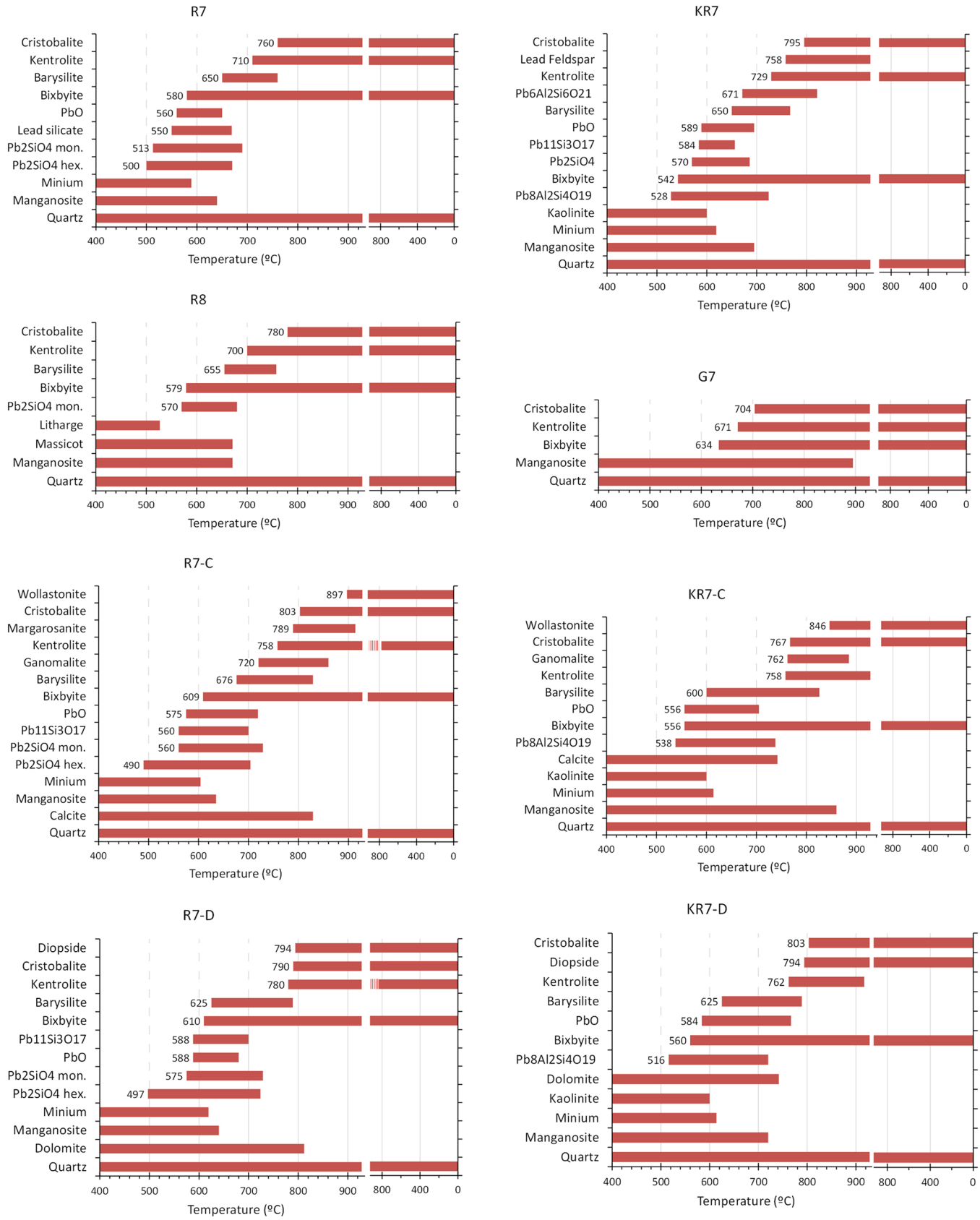

Fig. 7. Evolution of the phases formed during heating and cooling in the HT-PXRD experiments for all the mixtures studied.

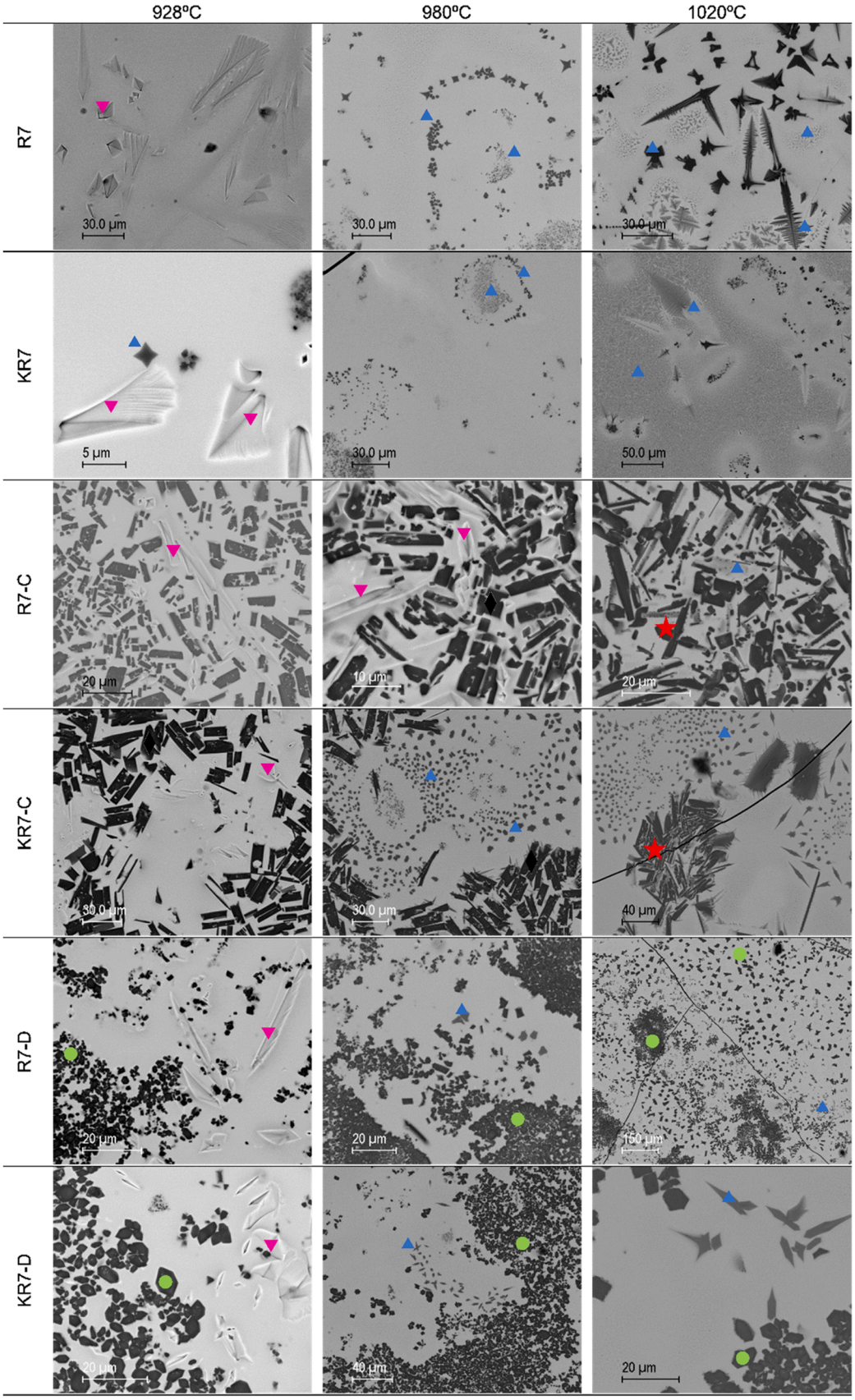

Fig. 8. Selection of BSE images taken for all the mixtures fired in the laboratory at 928 °C, 950 °C and 1020 °C. The phases formed are indicated with the same symbols and colours used in Figs. 2, 4 and 6. Blue triangles are braunite and red stars are bustamite.

materials and firing conditions used in the production of manganese decorated lead glazes. For this, a High Temperature Synchrotron Powder X-Ray Diffraction experiment (HT-PXRD) was designed to determine the manganese compounds formed during the heating and the cooling of a mixture of manganese oxide with a near eutectic high-lead glass composition; calcite, dolomite and kaolinite were also added to study their role in the manganese compounds formed. To expand the firing temperature range above the range accessible in the HT-PXRD experiment (928 °C) the same mixtures were also fired in the laboratory following the same thermal protocol at temperatures (690–1020 °C) and were analysed by Scanning Electron Microscopy (SEM).

The manganese phases which will be found in a high-lead glaze are kentrolite ($Pb_2Mn_2Si_2O_9$) (above 700 °C) and braunite (Mn_7SiO_{12}) (above 900 °C). Both are formed by the reaction of manganese oxide with the lead-silicate melt, and consequently, either whether a lead oxide and quartz mixture or a lead-silicate glass is used. Kentrolite melts above 900 °C and, if fired below 980 °C, recrystallises during the cooling with a different crystal habit (feather like instead of prismatic). Above 980 °C only braunite, which grows during the cooling (dendritic structure), is found. In the calcitic mixture the sequence ganomalite ($Pb_3(CaMn)_2Si_3O_{11}$), margarosanite ($Pb(Ca,Mn)_2Si_3O_9$) and wollastonite (above 850 °C) is observed while in the dolomitic mixture only diopsides are present at all temperatures. All these phases incorporate increasing amounts of manganese at higher temperatures, and at 1020 °C wollastonite incorporates enough manganese to transform into bustamite ($(Mn,Ca)_3Si_3O_9$). The presence of manganese in those phases leaves less manganese available for the crystallisation of kentrolite and braunite. Finally, barysilite ($(Pb,Mn)Si_2O_7$) is only expected in lead glazes fired at low temperature (below 850 °C). Relics of the manganese oxide particles can be found depending on their initial size appearing always as bixbyite (Mn_2O_3).

The presence and morphology of the manganese compounds found in high-lead glazes can be used to determine the firing conditions of traditional manganese decorations. The kinetic profile of the experiment is designed to provide the right sequence of manganese phases formed during heating and cooling, but not the exact temperature range which is heating rate dependent.

If the manganese content is low, once kentrolite is decomposed, there will not remain enough manganese in the melt to allow kentrolite recrystallisation and manganese will dissolve in the glaze completely. At higher temperatures, braunite will be found only if the melt contains enough manganese to produce some crystallites of braunite, otherwise, manganese will also dissolve in the glaze completely.

Declaration of Competing Interest

The authors declare that they have no known competing financial interests or personal relationships that could have appeared to influence the work reported in this paper.

Acknowledgments

J.M. and T.P. are grateful to the project PID2019-105823RB-I00 funded by the Ministerio de Ciencia e Innovación (Spain) and T.P. is grateful to Generalitat de Catalunya grant 2017SGR-0042. The experiments were performed at BL04 MSPD Beamline at ALBA Synchrotron Facility with the collaboration of Alba Staff, project number 2020094579.

Appendix A. Supporting information

Supplementary data associated with this article can be found in the online version at doi:10.1016/j.jeurceramsoc.2022.03.028.

References

[1] J. Molera, J. Coll, A. Labrador, T. Pradell, Manganese brown decorations in 10th to 18th century Spanish tin glazed ceramics, Appl. Clay Sci. 82 (2013) 86–90, https://doi.org/10.1016/j.clay.2013.05.018.
[2] T. Pradell, G. Molina, J. Molera, J. Pla, A. Labrador, The use of micro-XRD for the study of glaze color decorations, Appl. Phys. A Mater. Sci. Process. (2012) 121–127, https://doi.org/10.1007/s00339-012-7445-x.
[3] S. Coentro, L.C. Alves, C. Relvas, T. Ferreira, J. Mirão, J. Molera, T. Pradell, R.A. A. Trindade, R.C. da Silva, V.S.F. Muralha, The glaze technology of hispano-moresque ceramic tiles: a comparison between portuguese and Spanish collections, Archaeometry (2017), https://doi.org/10.1111/arcm.12280.
[4] M. Maggetti, SEM study of black, blue, violet and yellow inglaze colours of the oldest Swiss tin-opacified stove tiles (c.1450–c.1512, canton Bern), Archaeometry (2020), https://doi.org/10.1111/arcm.12638.
[5] L.F. Vieira Ferreira, D.P. Ferreira, D.S. Conceição, L.F. Santos, M.F.C. Pereira, T. M. Casimiro, I. Ferreira Machado, Portuguese tin-glazed earthenware from the 17th century. Part 2: A spectroscopic characterization of pigments, glazes and pastes of the three main production centers, Spectrochim. Acta Part A Mol. Biomol. Spectrosc. 149 (2015) 285–294, https://doi.org/10.1016/j.saa.2015.04.090.
[6] J. Molera, J.C. Carvajal López, G. Molina, T. Pradell, Glazes, colourants and decorations in early Islamic glazed ceramics from the Vega of Granada (9th to 12th centuries CE), J. Archaeol. Sci.: Rep. 21 (2018) 1141–1151, https://doi.org/10.1016/j.jasrep.2017.05.017.
[7] S. Coentro, J.M. Mimoso, A.M. Lima, A.S. Silva, A.N. Pais, V.S.F. Muralha, Multi-analytical identification of pigments and pigment mixtures used in 17th century Portuguese azulejos, J. Eur. Ceram. Soc. 32 (2012) 37–48, https://doi.org/10.1016/j.jeurceramsoc.2011.07.021.
[8] R. di Febo, J. Molera, T. Pradell, O. Vallcorba, J.C. Melgarejo, C. Capelli, Thin-section petrography and SR-μXRD for the identification of micro-crystallites in the brown decorations of ceramic lead glazes, Eur. J. Mineral. 29 (2017) 861–870, https://doi.org/10.1127/ejm/2017/0029-2638.
[9] B. Bajnóczi, G. Nagy, M. Tóth, I. Ringer, A. Ridovics, Archaeometric characterization of 17th-century tin-glazed Anabaptist (Hutterite) faience artefacts from North-East-Hungary, J. Archaeol. Sci. 45 (2014) 1–14, https://doi.org/10.1016/J.JAS.2014.01.030.
[10] G. Dorsam, A. Liebscher, B. Wunder, G. Franz, Crystal structures of synthetic melanotekite ($Pb_2Fe_2Si_2O_9$), kentrolite ($Pb_2Mn_2Si_2O_9$), and the aluminum analogue ($Pb_2Al_2Si_2O_9$), Am. Mineral. 93 (2008) 573–583, https://doi.org/10.2138/am.2008.2594.
[11] A. Silvestri, F. Nestola, L. Peruzzo, Manganese-containing inclusions in late-antique glass mosaic tesserae: a new technological marker? Minerals 10 (2020) 1–13, https://doi.org/10.3390/MIN10100881.
[12] M. Shevchenko, E. Jak, Experimental phase equilibria studies of the PbO–SiO_2 system, J. Am. Ceram. Soc. (2018) 458–471, https://doi.org/10.1111/jace.15208.
[13] W.R. Ott, M.G. McLaren, Subsolidus studies in the system PbO-SiO_2, J. Am. Ceram. Soc. 53 (1970), https://doi.org/10.1111/j.1151-2916.1970.tb12135.x.
[14] R.M. Smart, F.P. Glasser, Compound formation and phase equilibria in the system PbO-SiO_2, J. Am. Ceram. Soc. 57 (1974), https://doi.org/10.1111/j.1151-2916.1974.tb11416.x.
[15] R. di Febo, J. Molera, T. Pradell, J.C. Melgarejo, J. Madrenas, O. Vallcorba, The production of a lead glaze with galena: thermal transformations in the PbS–SiO_2 system, J. Am. Ceram. Soc. (2018), https://doi.org/10.1111/jace.15346.
[16] M. Shevchenko, E. Jak, Experimental liquidus study of the binary PbO-CaO and ternary PbO-CaO-SiO_2 systems, J. Phase Equilibria Diffus. (2019) 148–155, https://doi.org/10.1007/s11669-019-00705-3.
[17] M. Shevchenko, E. Jak, Thermodynamic optimization of the binary PbO–CaO and ternary PbO–CaO–SiO_2 systems, Calphad (2020), 101807, https://doi.org/10.1016/j.calphad.2020.101807.
[18] E. Jak, P.C. Hayes, The effect of the CaO/SiO_2 ratio on the phase equilibria in the ZnO-"Fe2O3"-(PbO + CaO + SiO_2) system in air: CaO/SiO_2 = 0.1, PbO/(CaO + SiO_2) = 6.2, and CaO/SiO_2 = 0.6, PbO/(CaO + SiO_2) = 4.3, Metall. Mater. Trans. B: Process. Metall. Mater. Process. Sci. 34 (2003), https://doi.org/10.1007/s11663-003-0064-3.
[19] S. Chen, B. Zhao, P.C. Hayes, E. Jak, Experimental study of phase equilibria in the PbO-Al_2O_3-SiO_2 system, Metall. Mater. Trans. B: Process. Metall. Mater. Process. Sci. 32 (2001), https://doi.org/10.1007/s11663-001-0088-5.
[20] A.E. Morris, A. Muan, Phase equilibria in the system MnO-Mn_2O_3-SiO_2, JOM 18 (1966), https://doi.org/10.1007/bf03378486.
[21] G. Eriksson, P. Wu, M. Blandert, A.D. Pelton, Critical evaluation and optimization of the thermodynamic properties and phase diagrams of the MnO-SiO_2 and CaO-SiO_2 systems, Can. Metall. Q. 33 (1994), https://doi.org/10.1179/cmq.1994.33.1.13.
[22] Y.B. Kang, I.H. Jung, S.A. Decterov, A.D. Pelton, H.G. Lee, Phase equilibria and thermodynamic properties of the CaO-MnO-Al_2O_3-SiO_2 system by critical evaluation, modeling and experiment, ISIJ Int. 44 (2004), https://doi.org/10.2355/isijinternational.44.975.
[23] T. Negas, C.A. Sorrell, Silica transformations in the system PbO-SiO_2, J. Am. Ceram. Soc. 51 (1968), https://doi.org/10.1111/j.1151-2916.1968.tb12632.x.
[24] S.J. Stevens, R.J. Hand, J.H. Sharp, Polymorphism of silica, J. Mater. Sci. 32 (1997), https://doi.org/10.1023/A:1018636920023.
[25] R. di Febo, L. Casas, Á.A. del Campo, J. Rius, O. Vallcorba, J.C. Melgarejo, C. Capelli, Recognizing and understanding silica-polymorph microcrystals in ceramic glazes, J. Eur. Ceram. Soc. 40 (2020), https://doi.org/10.1016/j.jeurceramsoc.2020.05.063.

[26] L. Fröberg, T. Kronberg, L. Hupa, M. Hupa, Influence of firing parameters on phase composition of raw glazes, J. Eur. Ceram. Soc. 27 (2007) 1671–1675, https://doi.org/10.1016/j.jeurceramsoc.2006.05.012.

[27] R. Casasola, J.M. Rincón, M. Romero, Glass-ceramic glazes for ceramic tiles: a review, J. Mater. Sci. 47 (2012) 553–582, https://doi.org/10.1007/S10853-011-5981-Y.

[28] R.J. Angel, Structural variation in wollastonite and bustamite, Mineral. Mag. 49 (1985) 37–48, https://doi.org/10.1180/minmag.1985.049.350.05.

[29] J. Abrecht, Stability relations in the system $CaSiO_3$-$CaMnSi_2O_6$-$CaFeSi_2O_6$, Contrib. Mineral. Petrol. 74 (1980) (1980) 253–260, https://doi.org/10.1007/BF00371695.

[30] Stacking Variations and Nonstoichiometry in the Bixbyite-braunite Polysomatic Mineral Group, Am. Mineral. 74 (11–12) (1989) 1325–1336. 〈https://pubs.geoscienceworld.org/msa/ammin/article-abstract/74/11-12/1325/42207/Stacking-Variations-and-Nonstoichiometry-in-the〉. accessed December 13, 2021.